Construction of Highway Bridge Health Monitoring and Vehicle-Mounted Intelligent Operation and Maintenance System Based on Edge Computing Joint Clustering Algorithm

(IJCSNT) International Journal of Communication Systems and Network Technologies
ISSN Number: 2053-6283
Volume 14, Issue No. 1, 20–31
©The Author(s) 2025
https://journals.mirlabs.in/index.php/ijcsnt
DOI-10.18486/ijcsnt/14.1.003
IJCSNT

Donghong Xue[1], Guijuan Tian[2], Yingchuan Lv[3], Yamei Zhou[4]

Abstract

To address the bottlenecks of hidden and sudden structural damage to highway bridges under long-term heavy traffic, the inability of traditional central cloud monitoring to process massive amounts of vehicle-mounted mobile data in real time, and the difficulty in multi-source heterogeneous data fusion, this paper constructs a health monitoring and vehicle-mounted intelligent operation and maintenance system driven by edge computing and joint clustering. First, a three-layer collaborative architecture of “vehicle-roadside-edge cloud” is designed. Then, a distributed multi-view joint clustering algorithm is proposed, simultaneously optimizing bidirectional clustering of sample and sensor features, and exchanging centroids only through federated averaging between edge nodes. Finally, a vehicle-mounted terminal is developed to map damage level and location in real time to graded early warning and maintenance suggestions. Experiments show that the anomaly detection accuracy is 94.7%, alarm latency is 87ms, transmission volume is 0.41MB, a reduction rate of over 99.6%, and strong noise robustness. The integration of edge computing and joint clustering solves the problems of real-time performance and data silos, achieving low-latency and high-precision vehicle-mounted structural health operation and maintenance.

Keywords

Structural Health Monitoring, Edge Computing, Joint Clustering, Damage Identification, Vehicle-mounted Maintenance

Received: 26 December 2024; **Revised:** 03 April 2025; **Accepted:** 20 April 2025;
Published: 30 April 2025;

[1, 2, 3, 4]Shandong Transport Vocational College, Tai’an, Shandong, China.

Corresponding author:
Email: 17662366817@163.com

Introduction

In recent years, under the coupled effects of long-term heavy traffic and complex environment, the structural damage of highway bridges and roads has become increasingly hidden and sudden, posing a severe challenge to operational safety[1]. Traditional structural health monitoring relies heavily on the centralized aggregation and offline analysis of massive sensor data in the central cloud, which is difficult to meet the stringent requirements of millisecond-level real-time alarms and efficient fusion of multi-source heterogeneous information in vehicle-mounted mobile scenarios. Moreover, the large-scale transmission of raw data brings bandwidth load and privacy risks[2,3]. Exploring a new paradigm that completes real-time computation at the edge and achieves collaborative knowledge discovery among multiple nodes has important theoretical significance and engineering application value for improving the timeliness and intelligence level of bridge and road monitoring.

To overcome the aforementioned bottlenecks, this paper completed the following main tasks: A three-layer collaborative edge computing architecture of "vehicle-roadside-edge cloud" is constructed, migrating signal denoising and feature extraction tasks to edge nodes, thus reducing data redundancy at the source; a distributed multi-view joint clustering algorithm is proposed, fusing multi-source sensor features without sharing original data to achieve autonomous discovery of damage patterns and accurate classification of safety levels; an in-vehicle intelligent operation and maintenance terminal is developed, mapping analysis results to hierarchical early warning and maintenance suggestions in real time, forming a complete closed loop from sensor acquisition to decision response. Multiple sets of experiments verified the comprehensive advantages of the proposed system in terms of detection accuracy, response latency, and communication efficiency. The paper is organized as follows: the introduction introduces the research background and related work; the methodology section details the architecture design and key algorithm implementation of the edge computing joint clustering system; the experimental section provides multi-dimensional experimental evaluation and result analysis; and the conclusion summarizes the entire paper and looks forward to future research directions.

Related Work

Regarding the issue of health monitoring of highway bridges, existing research mainly focuses on sensor deployment, structural response analysis, damage identification models, and cloud monitoring platforms. Bao and Li systematically summarized the data-driven modeling method in structural health monitoring from the perspective of machine learning paradigm, pointing out that machine learning can extract damage features from complex structural response data[4]. Malekloo et al. further discussed the application of high-dimensional sensing data, intelligent sensing technology, and machine learning in structural health monitoring[5]. For bridge scenarios, Zinno et al. reviewed the progress of artificial intelligence in bridge structural health monitoring[6]. Hou et al. combined the BIM visualization management system with the LSTM network to realize the visualization early warning of structural health monitoring data[7]. Wang et al. pointed out that the combination of data fusion and machine learning helps to improve the accuracy and reliability of complex engineering structure status assessment[8]. The above studies still have problems such as the strong dependence of the central cloud model on network bandwidth and computing resources, making it difficult to meet the millisecond-level early warning requirements in vehicle scenarios.

To address the above problems, edge computing and cluster analysis provide new solutions for highway and bridge health monitoring. Qiu et al. analyzed the development trend of edge computing from the perspective of structural health monitoring, pointing out that the computing task should be pushed down to the edge node close to the data source[9]. Anaissi et al. proposed a personalized federated learning framework for damage detection in structural health monitoring[10]. Cheema et al. further proposed a cluster federated learning method for group structural health monitoring, which improved the damage identification capability in heterogeneous structural environments[11]. Most of the above research methods have not been fully applied to vehicle-mounted mobile sensing scenarios, and few have considered the collaborative clustering relationship between structural state samples and sensor features at the same time. Based on this, this paper introduces edge computing combined with distributed multi-view clustering algorithm to construct a vehicle-mounted intelligent operation and maintenance system for highway and bridge health monitoring, so as to achieve low latency, multi-source fusion and cross-edge node collaborative structural safety assessment.

Method

Deployment of a Three-Tier Collaborative Architecture of "Vehicle-Roadside-Edge Cloud"

The "vehicle-roadside-edge cloud" three-layer collaborative architecture decentralizes data processing from the central cloud to the network edge, minimizing the distance between computation and data sources. It compresses redundancy and shortens response links at the source, balancing global collaboration with node autonomy. The architecture consists of three functional layers from bottom to top: The vehicle-side architecture embeds edge computing units within the operating vehicle, synchronously collecting multi-source signals such as vibration, strain, and displacement. It performs adaptive wavelet denoising locally and extracts compact features such as power spectral entropy, peak frequency, and kurtosis, compressing 10-second raw waveforms into several KB of statistics. After initial anomaly screening, feature vectors, locations, and timestamps are submitted to the roadside architecture only via 5G or a backup DSRC link when features deviate from the safety envelope. The roadside architecture deploys an edge computing industrial control computer cluster, responsible for receiving and time-aligning asynchronous data streams from multiple vehicles. It iteratively performs distributed multi-view joint clustering locally using historical and real-time samples, updating the centroid of local damage patterns. Only the centroid parameters are transmitted back to the edge cloud via fiber optic cable for federated aggregation. Simultaneously, it maintains a real-time database of bridge safety status at this node, supporting millisecond-level local alarm queries.

The top-level edge cloud aggregates the local centroids of each roadside node, uses federated average safe aggregation to generate a global clustering model, and distributes the global centroids back to each node to start the next iteration. Throughout the federated loop, the original data never leaves the local machine. The edge cloud also uses long-period centroid drift trajectories to assess the damage accumulation rate, dynamically adjusts the graded early warning thresholds, and pushes alarm rules and maintenance suggestions to the vehicle-mounted terminal. The three layers collaborate through differentiated networks: the vehicle-roadside link uses 5G/DSRC to ensure low-latency mobile access, while the roadside-edge cloud relies on a dedicated fiber optic network for reliable exchange of lightweight centroid parameters.

Local Denoising and Feature Extraction of Multi-Source Sensor Signals

The signal types involved in bridge and road monitoring mainly include bridge deck vibration acceleration, dynamic strain of key sections, support displacement, and slow variables such as temperature. Vibration and strain signals are sensitive to local structural damage, but are easily contaminated by vehicle engine vibration, high-frequency bumps caused by uneven road surfaces, and electromagnetic coupling noise. Therefore, a discrete wavelet transform denoising method based on adaptive thresholds is used to preprocess the above dynamic signals. Specifically, the “db6” wavelet basis, which is tightly supported and matches the impact response waveform well, is selected, and a 5-level wavelet packet decomposition is performed on the 10 s time window signal intercepted by a single channel. At each decomposition scale, the shrinkage threshold of the detail coefficients of each level is adaptively determined using the Stein unbiased risk estimation criterion, and the threshold is defined as (1):

$$\mathrm{T_j} = \sigma_\mathrm{j}\sqrt{2\log \mathrm{N_j}} \cdot \gamma_\mathrm{j} \tag{1}$$

In the formula, σ_j is the noise standard deviation estimate of the j-th layer detail coefficient, $\mathrm{N_j}$ is the coefficient length of the layer, and γ_j is the SURE criterion adaptive shrinkage factor. Coefficients below the threshold are subjected to soft thresholding to zero, while coefficients above the threshold are retained or compressed proportionally. Finally, the time domain signal after noise reduction is reconstructed by wavelet inverse transform. For slowly varying signals such as displacement and temperature, sliding median filtering is used to remove occasional pulse interference, and first-order differential detection is used to remove abnormal jump points caused by instantaneous power failure of the sensor[12].

After noise reduction, the time domain waveforms of each sensing channel still have high dimensionality, and the amplitude scales of different physical quantities vary greatly. It is necessary to further extract statistical features that are sensitive to damage and robust to the operating environment. This system extracts four frequency domain features for vibration acceleration signals: power spectral entropy, which is used to quantify the complexity of the signal spectrum structure. Its calculation formula is (2):

$$\mathrm{H} = -\sum_{\mathrm{k}=1}^{\mathrm{K}} \mathrm{p_k}\log \mathrm{p_k}, \quad \mathrm{p_k} = \frac{\mathrm{S(f_k)}}{\sum_{\mathrm{i}=1}^{\mathrm{K}} \mathrm{S(f_i)}} \tag{2}$$

$\mathrm{S(f_k)}$ is the power spectrum value estimated by the Welch method at the k-th frequency bin. When micro-damage occurs in the structure, it is usually accompanied by energy redistribution in a specific frequency band, and the entropy value will shift. The main peak frequency and main peak amplitude of the frequency response function are estimated by the Welch average periodogram method to estimate the power spectral density of the signal. The frequency corresponding to the maximum spectral peak in the range of 0.5∼40 Hz and its normalized amplitude are automatically searched. This parameter is more sensitive to stiffness degradation and boundary constraint changes. At the same time, three time-domain features are added: kurtosis is as follows (3):

$$\mathrm{K} = \frac{1}{\mathrm{M}}\sum_{\mathrm{m}=1}^{\mathrm{M}} \left(\frac{\mathrm{x_m} - \mu}{\sigma}\right)^4 \tag{3}$$

It is extremely sensitive to the impact component in the signal and can capture sudden events such as crack opening and closing; the root mean square value reflects the total energy level of the signal and is directly related to the traffic load intensity; the waveform factor is as follows (4):

$$W = \frac{\sqrt{\frac{1}{M}\sum_{m=1}^{M} x_m^2}}{\frac{1}{M}\sum_{m=1}^{M} |x_m|} \tag{4}$$

It is used to measure the degree of waveform spikes, aiding in the differentiation of damage types. x_m represents the discrete sampling points of the time-domain signal after noise reduction, and μ and σ are its mean and standard deviation, respectively. For dynamic strain signals, the feature extraction logic is similar to that for vibration, but the search range for the main frequency peak is narrowed to 0.1–10 Hz to match the quasi-static characteristics of the strain response. Since displacement signals mainly reflect the low-frequency trend of support deformation, only the mean drift and standard deviation are extracted to monitor the development of irreversible deformation. All features are Z-score standardized at the channel level after extraction, unifying the numerical distribution across different sensors to a zero-mean unit variance space.

Distributed Multi-View Joint Clustering Algorithm for Damage Pattern Discovery

After local noise reduction and feature extraction of multi-source signals are completed at the vehicle-mounted and roadside terminals, each edge node holds a compact feature description of the structural state sample. However, a single node can only observe a local area's sensor view, making it difficult to comprehensively characterize the overall damage pattern of the bridge. This section describes the design concept and execution flow of the distributed multi-view joint clustering algorithm, enabling autonomous discovery of multi-view damage patterns without transmitting original data. Figure 1 illustrates the damage pattern discovery process.

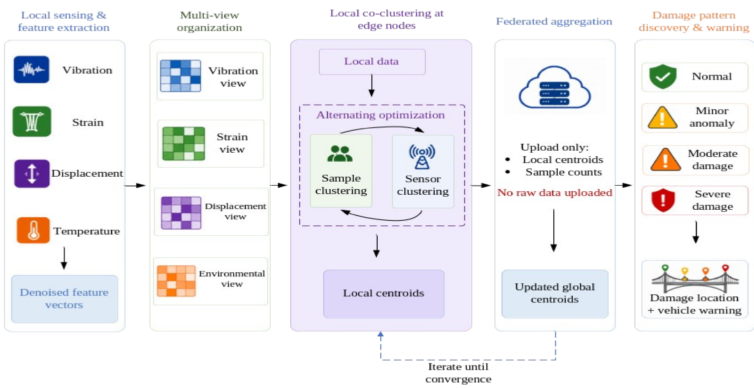

Figure 1. Schematic diagram of the distributed multi-view joint clustering damage pattern discovery process

The algorithm adopts a bidirectional graph regularized joint clustering optimization objective in mathematical form. Let the sample feature matrix be X, the sample clustering indicator matrix be U, the sensor clustering indicator matrix be V, and the joint centroid matrix be C, then the objective function is (5):

$$\min_{\mathrm{U,V,C}} \left\|\mathrm{X} - \mathrm{UCV}^{\mathrm{T}}\right\|_{\mathrm{F}}^{2} + \lambda\,\mathrm{tr}\left(\mathrm{U}^{\mathrm{T}}\mathrm{L}_{\mathrm{V}}\mathrm{U}\right) + \mu\,\mathrm{tr}\left(\mathrm{V}^{\mathrm{T}}\mathrm{L}_{\mathrm{U}}\mathrm{V}\right) \tag{5}$$

Where L_{U} and L_{V} are the graph Laplacian matrices of the sample side and the sensor side, respectively, and λ and μ are regularization coefficients. The first term measures the joint clustering reconstruction error, and the latter two terms force the smoothness of the sample clustering structure and the sensor clustering structure on their respective graphs and couple them together[13]. This form extends the traditional K-means to bidirectional collaborative clustering, so that the discovery of damage patterns depends not only on the feature distribution of the samples themselves, but also on the functional association between sensors. Thus, the synchronous mining of the "damage-sensor" bidirectional structure is realized. The key parameters and convergence conditions involved in the algorithm execution are shown in Table 1.

Table 1. Key parameters and convergence conditions of the distributed multi-view co-clustering algorithm

Parameter/Condition	Value	Description
Number of clusters K	4	Corresponding to four structural safety levels
Maximum local iterations	50	Upper limit of local updates per round
Maximum global aggregation rounds	200	Upper limit of federated communication rounds
Local convergence threshold	$< 10^{-4}$	Objective function decrease magnitude
Aggregation strategy	Weighted federated averaging	Weights proportional to cluster sample counts
Communication payload	Centroid parameters + sample counts	∼0.4 KB per node per transmission

The objective function is solved using a block-based iterative strategy within the framework of the alternating direction multiplier method. Each global iteration includes two local updates and one global aggregation. The first step is to fix the sensor function cluster partition and update the sample cluster: the centroid update formula for the sample of local node i in the t-th round of local iteration is (6):

$$\mathrm{c}_{\mathrm{k}}^{(\mathrm{i},\mathrm{t}+1)} = \frac{\sum_{\mathrm{n}\in\mathrm{N}_{\mathrm{k}}^{(\mathrm{i})}} \mathrm{x}_{\mathrm{n}}}{\left|\mathrm{N}_{\mathrm{k}}^{(\mathrm{i})}\right|}, \quad \mathrm{N}_{\mathrm{k}}^{(\mathrm{i})} = \left\{\mathrm{n} \mid \mathrm{u}_{\mathrm{nk}}^{(\mathrm{i},\mathrm{t})} = 1\right\} \tag{6}$$

Wherein, $\mathrm{c}_{\mathrm{k}}^{(\mathrm{i},\mathrm{t}+1)}$ represents the centroid of the sample in the damage mode; $\mathrm{N}_{\mathrm{k}}^{(\mathrm{i})}$ represents the set of samples in node i that are divided into the k-th class; $\mathrm{u}_{\mathrm{nk}}^{(\mathrm{i},\mathrm{t})}$ represents the clustering label in the iteration. Each edge node takes the local cached samples and real-time features as input, initializes with the joint centroid matrix distributed globally, and alternately performs two steps of local optimization: sample clustering and sensor functional cluster division. First, the hard allocation of samples is completed based on Euclidean distance and the centroid of the samples is updated. Then, the centroid of the sensor cluster is updated according to the response distribution of the sensor in each damage mode. This continues until the objective function converges or the maximum number of local iterations is reached. Then, only the centroid of the sample cluster, the centroid of the sensor cluster, and the number of samples in the corresponding cluster are uploaded to the edge cloud for federated weighted average aggregation. After the global centroid is safely distributed, the next round of loop is triggered. Throughout the process, the original data and labels remain locally. After convergence, each global sample centroid is automatically interpreted as a composite damage mode such as vibration energy rise and strain drift. The system divides the safety level into four levels from normal to severe damage. New samples are mapped to the corresponding level in real time through the shortest centroid distance[14,15].

Real-time Hierarchical Alarm Mapping of Vehicle-Mounted Intelligent Operation and Maintenance Terminal

The vehicle-mounted intelligent operation and maintenance terminal transmits the analysis results of edge-side joint clustering to drivers and maintenance units in real time, forming the final closed loop from damage detection to decision-making and response. The terminal maintains communication with roadside nodes via 5G or DSRC links, automatically registers when a vehicle enters the monitoring area, and receives a truncated safety status data packet containing only the safety level code, damage interval marker, alarm level, and speed limit or detour suggestions, with each packet controlled to be in the hundreds of bytes. Based on the four levels of results output by joint clustering—normal, minor anomaly, moderate damage, and severe damage—the terminal executes a three-level response: In normal condition, a green silent display is maintained; in minor anomaly condition, a yellow light breathing effect and low-frequency voice prompts are triggered, simultaneously displaying distance and suggested speed limits; in moderate damage condition, an orange high-contrast interface and periodic buzzer alarms are activated, and an event snapshot is transmitted back; in severe damage condition, a full-screen red warning is displayed, emergency information is broadcast with the highest priority, and a brake pre-tensioning signal is sent to the vehicle's CAN bus. Event logs are reported via satellite short messages and cellular dual links to ensure communication reliability. Furthermore, when a continuous drift of the damage pattern's centroid is detected but has not yet reached the threshold, the terminal pushes an inspection suggestion via a trip-end information card and generates a maintenance priority list weighted by drift rate and safety level. The software implementation employs a multi-threaded real-time system, with a response latency of less than 50 ms for the three-level alarm threads. The human-machine interface follows a low cognitive load principle, presenting a three-segment high-contrast text format: "Problem Location Suggestion." Voice parameters have been calibrated on a real vehicle to prevent confusion with conventional in-vehicle audio.

Results and Discussion

Experimental Setup

(1) Experimental Data and Operating Conditions

Based on long-term monitoring data of a cross-river highway bridge from June 2023 to May 2024, 386 measuring points from 14 types of sensors, including bridge deck vibration acceleration, dynamic

strain, and support displacement, are collected. Four typical operating conditions—normal operation, minor damage, moderate damage, and severe damage—were extracted from the raw data. Each condition contained 3000 multi-source signal segments, each 10 seconds long, divided into training, validation, and test sets in a 7:1:2 ratio. When simulating a vehicle-mounted scenario, vehicle engine vibration noise and random road bumps are superimposed, with the signal-to-noise ratio gradually varying from 5dB to 30dB.
(2) Edge Computing Experimental Platform

The vehicle-mounted edge unit adopts an embedded platform based on ARM Cortex-A78 (8 cores, 16GB memory), the roadside edge nodes are deployed on an Intel Core i7-13700H industrial control computer, and the edge cloud server is configured with NVIDIA Jetson AGX Orin. The nodes are networked through a hybrid network of 5G private network and fiber optic, with bandwidth set at 100 Mbps uplink and 500 Mbps downlink, and a simulated latency of 5$\sim$10ms.
(3) Algorithm Parameters and Training Configuration

Adaptive wavelet thresholding denoising uses the “db6” wavelet basis with 5 decomposition layers; after feature extraction, each sensor node retains a 6-dimensional sensitive feature vector (power spectral entropy, frequency response function peak frequency and amplitude, kurtosis, root mean square value, waveform factor). Joint clustering initializes the federated cluster number K=4, with a local maximum iteration count of 50 and a global federated aggregation round count of 200. The FedAvg safe aggregation strategy is adopted, and local data is not shared among edge nodes.

Experimental Analysis

a) Anomaly Detection Accuracy and Alarm Delay Experiment

To evaluate the overall performance of this system in terms of detection accuracy and real-time response, a test set of 2400 samples across four operating conditions, collected synchronously from 80 vehicle terminals, is selected. Three methods are run under a unified edge node and 5G private network: cloud-based LSTM anomaly detection (extracting temporal features at the edge and uploading them to the cloud for classification), federated K-means clustering (independent clustering at each node, with centroids uploaded to the server for federated averaging), and the distributed multi-view joint clustering method presented in this paper. Anomaly detection accuracy is recorded, and the end-to-end latency from edge node discrimination to vehicle terminal alarm triggering is measured using NTP timestamps. The actual data transmission volume during the inference phase for each method is also statistically analyzed.

array

Table 2. Comparison of anomaly detection accuracy and alarm latency

ccc

Method	Anomaly Detection Accuracy (%)	End-to-End Alert Latency (ms)	Data Transmission Volume (MB)
Cloud-based LSTM anomaly detection	90.8	265.4	184.6
Federated K-means clustering	91.5	116.2	0.38
Proposed distributed multi-view co-clustering	94.7	87	0.41

As shown in Table 2, the anomaly detection accuracy of the proposed joint clustering method reaches 94.7%, which is 3.9 and 3.2 percentage points higher than that of cloud-based LSTM and federated K-means, respectively. The end-to-end latency for key alarms is only 87.0 ms, which is 32.8% of that of the cloud-based solution and 25.1% shorter than that of federated K-means. The data transmission volume of the proposed method is only 0.41 MB, which is at an extremely low level, similar to that of federated K-means, while cloud-based LSTM requires 184.6 MB of transmission. The data reduction rate of the proposed method is 99.78% compared to the cloud-based solution. The results show that multi-view joint clustering, while maintaining the advantage of lightweight edge transmission, deeply integrates heterogeneous features, achieving a balance between high accuracy and low latency, and its overall performance is significantly better than the two advanced mainstream solutions.

b) Evaluation Experiment on the Relationship between Latency and Data Reduction and Vehicle Density

To evaluate the real-time performance and communication efficiency of the system under large-scale vehicle terminal access, the number of terminals is increased sequentially from 10 to 80, with each terminal continuously transmitting 10-second multi-source sensor segments. Under unified edge node and 5G private network conditions, the distributed multi-view joint clustering scheme and the cloud-based LSTM anomaly detection scheme proposed in this paper are run respectively. The end-to-end latency of key alarms at each scale is recorded, and the data transmission volume reduction rate is calculated based on the transmission volume of the cloud-based scheme. The experiment is repeated 5 times, and the average value is taken.

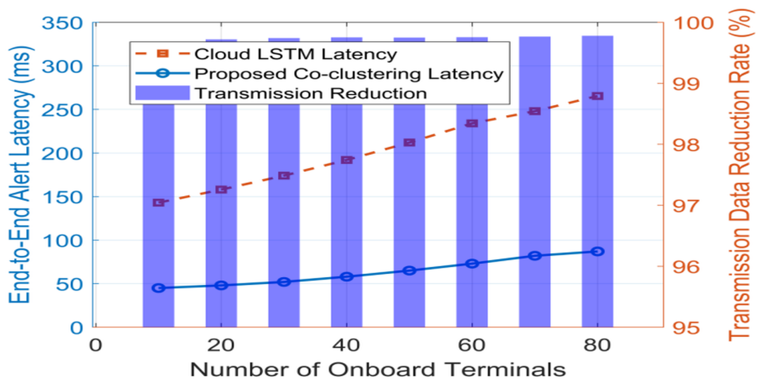

Figure 2. Assessment of the relationship between latency and data reduction and vehicle density

In Figure 2, as the number of vehicle terminals increases from 10 to 80, the end-to-end latency of the key alarm in our proposed solution only gradually increases from 45ms to 87ms, while the cloud-based LSTM solution increases from 143ms to 265ms. Our proposed latency consistently remains below one-third of the cloud-based solution, demonstrating a significant advantage in real-time response. Regarding the amount of data transmitted, our proposed solution maintains a data reduction rate of over 99.6% compared to the cloud-based solution; with 80 terminals, only 0.41MB needs to be transmitted, far lower than the 184.6MB of the cloud-based solution. It is evident that through edge collaboration and lightweight centroid switching, the system maintains millisecond-level alarms while introducing almost no additional bandwidth overhead, meeting the stringent requirements of high-density vehicle monitoring for real-time performance and communication efficiency.

c) Stability Experiment of Anomaly Detection Accuracy

To verify the robustness of the proposed method in a vehicle-mounted environment with strong interference, Gaussian white noise with a signal-to-noise ratio ranging from 5dB to 30dB is superimposed on the test samples to simulate signal degradation caused by road bumps and electromagnetic interference. Four structural damage conditions—normal, minor, moderate, and severe—were selected, and distributed multi-view joint clustering is repeatedly performed 50 times at each noise level. The average anomaly detection accuracy for each condition is recorded to examine the method's recognition stability as sensor data quality continuously deteriorates. See Figure 3 for details.

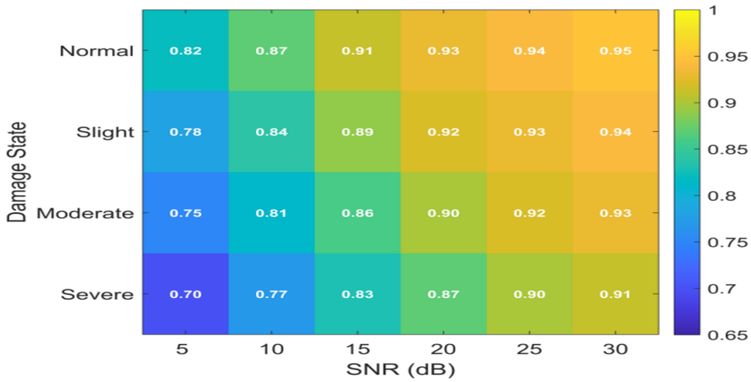

Figure 3. Stability assessment of anomaly detection accuracy

At an extremely low signal-to-noise ratio (SNR) of 5 dB, the proposed method maintains a 70% accuracy rate for detecting severe damage, and 82%, 78%, and 75% for normal, minor, and moderate damage, respectively. When the SNR increases to 30 dB, the accuracy rates for all four structural states exceed 91%, with 95% for normal conditions and 94% for minor damage. The maximum fluctuation across all operating conditions is only 21 percentage points, and no accuracy drop occurs due to increased noise. The results demonstrate that distributed multi-view joint clustering exhibits strong resistance to sensor signal degradation and can stably identify structural damage patterns even in environments with strong vehicle vibration and electromagnetic interference.

Conclusion

This paper addresses the core issues of insufficient real-time performance and difficulties in multi-source data fusion in highway and bridge health monitoring, and constructs an onboard intelligent operation and maintenance system driven by edge computing and joint clustering. By employing a three-layer collaborative edge architecture, computational tasks are decentralized to onboard and roadside nodes. Combined with a distributed multi-view joint clustering algorithm, accurate identification of damage patterns and safety level classification are achieved without sharing original data, forming a complete closed loop from sensor acquisition and edge analysis to tiered early warning. Experiments verify the system's comprehensive advantages in detection accuracy, alarm latency, and communication efficiency. However, this study only validated the system on a limited number of bridges and under fixed operating conditions; its generalization ability to extreme disaster scenarios needs further investigation.

The consistency guarantee of the algorithm when deployed on a larger scale of nodes requires further exploration. Future work will focus on adaptive upgrades of multimodal fusion and cross-bridge transfer learning to further improve the system's robustness and scalability in complex road network environments.

Author Contributions

The corresponding author is Guijuan Tian.

References

[1] Rizzo P, Enshaeian A. Bridge health monitoring in the United States: A review[J]. Structural Monitoring and Maintenance, 2021, 8(1): 1-50. DOI: 10.12989/smm.2021.8.1.001.

[2] Malekjafarian A, Corbally R, Gong W. A review of mobile sensing of bridges using moving vehicles: Progress to date, challenges and future trends[J]. Structures, 2022, 44(1): 1466-1489. DOI: 10.1016/j.istruc.2022.08.075.

[3] Shokravi H, Vafaei M, Samali B, Bakhary N. In-fleet structural health monitoring of roadway bridges using connected and autonomous vehicles' data[J]. Computer-Aided Civil and Infrastructure Engineering, 2024, 39(14): 2122-2139. DOI: 10.1111/mice.13180.

[4] Bao Y, Li H. Machine learning paradigm for structural health monitoring[J]. Structural Health Monitoring, 2021, 20(4): 1353-1372. DOI: 10.1177/1475921720972416.

[5] Malekloo A, Ozer E, AlHamaydeh M, Girolami M. Machine learning and structural health monitoring overview with emerging technology and high-dimensional data source highlights[J]. Structural Health Monitoring, 2022, 21(4): 1906-1955. DOI: 10.1177/14759217211036880.

[6] Zinno R, Haghshenas S S, Guido G, Vitale A. Artificial Intelligence and Structural Health Monitoring of Bridges: A Review of the State-of-the-Art[J]. IEEE Access, 2022, 10(1): 88058-88078. DOI: 10.1109/ACCESS.2022.3199443.

[7] Hou G, Li L, Xu Z, Chen Q, Liu Y, Qiu B. A BIM-Based Visual Warning Management System for Structural Health Monitoring Integrated with LSTM Network[J]. KSCE Journal of Civil Engineering, 2021, 25(8): 2779-2793. DOI: 10.1007/s12205-021-0565-0.

[8] Wang H, Barone G, Smith A. Current and future role of data fusion and machine learning in infrastructure health monitoring[J]. Structure and Infrastructure Engineering, 2024, 20(12): 1853-1882. DOI: 10.1080/15732479.2023.2165118.

[9] Qiu S, Malik M, Ehsan H, Wang W, Wang J, Cheng R, Wei W, Zaheer Q. Trends and perspectives in structural health monitoring through edge computing: A review with zero-shot natural language processing categorization[J]. Journal of Railway Science and Technology, 2025, 1(2): 59-74. DOI: 10.1016/j.jrst.2025.08.003.

[10] Anaissi A, Suleiman B, Alyassine W. Personalised federated learning framework for damage detection in structural health monitoring[J]. Journal of Civil Structural Health Monitoring, 2023, 13(1): 295-308. DOI: 10.1007/s13349-022-00615-y.

[11] Cheema M A, Sarwar M Z, Cantero D, Rossi P S. Clustered Federated Learning for Population-Based Structural Health Monitoring[J]. IEEE Internet of Things Journal, 2025, 12(13): 24958-24967. DOI: 10.1109/JIOT.2025.3556670.

[12] Li Z, Lin W, Zhang Y. Drive-by bridge damage detection using Mel-frequency cepstral coefficients and support vector machine[J]. Structural Health Monitoring, 2023, 22(5): 3302-3319. DOI: 10.1177/14759217221150932.

[13] Favarelli E, Testi E, Giorgetti A. The impact of sensing parameters on data management and anomaly detection in structural health monitoring[J]. Journal of Civil Structural Health Monitoring, 2022, 12(6): 1413-1425. DOI: 10.1007/s13349-022-00566-4.

[14] Vivekanand Aloji, Parashuram L, Amar R D, Sunil Kumar, ”Mechanical Properties of Glass Fibre Reinforced Concrete using Jhama Bricks as Fine Aggregate Replacement”, International Journal of Communication Systems and Network Technologies, Vol.10, No.1, pp.17-41, 2021. DOI-10.18486/ijcsnt/10.1.128

[15] Sarmadi H, Entezami A, Salar M, De Michele C. Bridge health monitoring in environmental variability by new clustering and threshold estimation methods[J]. Journal of Civil Structural Health Monitoring, 2021, 11(3): 629-644. DOI: 10.1007/s13349-021-00472-1.